AIAA JOURNAL
Vol. 49, No. 2, February 2011

Technical Notes

Preliminary Assessment of Two-Fluid Model for Direct Numerical Simulation of Particle-Laden Flows

Babak Shotorban*
University of Alabama in Huntsville, Huntsville, Alabama 35899

DOI: 10.2514/1.J050721

I. Introduction

PARTICLE-LADEN flows can be described through two approaches of trajectory and two-fluid [1]. In the trajectory approach, particles are individually tracked in the Lagrangian frame. In the two-fluid approach, particles are treated just as another fluid through model equations in the Eulerian frame. The model development is performed via approaches similar to that in the kinetic theory of gases where molecules are statistically dealt with leading to differential equations representing the gas as a continuum media. In practical situations the number of particles could be so large that tracking each particle computationally is not feasible due to limitations in current computers; therefore, simulations based on trajectory models are not feasible for flows with a very large number of particles. In fact, for the quantification of concentration (number density) of particles in the trajectory approach, practically a large number of particles per cell is required to generate enough samples. On the other hand, in the two-fluid approach, much more sophisticated models are required due to closure problems resulting from the statistical averaging.

There are various two-fluid models for dealing with particle-laden flows [2–10]. In the current work we adapt the two-fluid model proposed by Pandya and Mashayek [11] for the large-eddy simulation of turbulence to a case in which the filter size is taken so small that all scales of the fluid phase velocity are resolved. This adaptation can be thought as a two-fluid formulation for direct numerical simulation (DNS) of turbulent or laminar flows. It is noted that we consider the case of particles much smaller than scales of undisturbed motion that would exist in the absence of particles. When particles are present it is unavoidable that the fluid motion will have length scales comparable to those of the particle. Thus a *true DNS* of the fluid is not possible; though, in the current work by DNS we mean full-scale simulations of the fluid phase where *point-particle* assumption is made for particles [12–14]. In this work, for the assessment purposes the model is simplified to a one-dimensional case for which a sample problem is solved.

II. Two-Fluid Model Description

The governing equations of the position vector $\mathbf{X} = (X_1, X_2, X_3)$ and velocity vector $\mathbf{V} = (V_1, V_2, V_3)$ of a particle in the Lagrangian frame are

$$\frac{\mathrm{d}X_i}{\mathrm{d}t} = V_i \tag{1}$$

$$\frac{\mathrm{d}V_i}{\mathrm{d}t} = \frac{f_1}{\tau}(U_i^* - V_i) \tag{2}$$

where $\tau = Re_f \rho_p d^2/18$ with d and ρ_p denoting the particle diameter and density, respectively, is the particle time constant [1]. All variables are normalized by reference length L_f, density ρ_f, and velocity. $Re_f = \rho_f U_f L_f/\mu$ is the reference Reynolds number. Superscript $*$ shows the value of a carrier phase variable at the location of the particle, i.e., $U_i^*(t) = U_i(\mathbf{X}(t), t)$ where U_i is the velocity vector component of the carrier phase at i direction. Coefficient f_1 is a function of the Reynolds number of the particle $Re_p = Re_f \rho^* |\mathbf{U}^* - \mathbf{V}| d$ where at the limit of a small Re_p, it is $f_1 = 1$ [1], which is the value that we consider in this study. It is noted that particles with a larger Stokes number, which is a nondimensional number defined as the ratio of the particle time constant and the smallest scale of the fluid flow (Kolmogorov time scale in the case of turbulence), possess high inertia leading to larger deviations between the velocities of particles and their surrounding fluid velocities, which, in turn, results in higher particle Reynolds numbers. Thus, setting $f_1 = 1$ does not seem to be a good approximation for very large Stokes numbers.

It can be shown that $W(\mathbf{x}, \mathbf{v}, t)$, which is called the fine-grained phase-space density [11] and defined by

$$W(\mathbf{x}, \mathbf{v}, t) = \delta(\mathbf{x} - \mathbf{X}(t))\delta(\mathbf{v} - \mathbf{V}(t)) \tag{3}$$

where $\mathbf{x} = (x_1, x_2, x_3)$ and $\mathbf{v} = (v_1, v_2, v_3)$, satisfies the Liouville equation of the fine-grained phase-space density

$$\frac{\partial W}{\partial t} + \frac{\partial v_i W}{\partial x_i} - \frac{\partial}{\partial v_i}\left[\frac{(v_i - u_i)}{\tau} W\right] = 0 \tag{4}$$

where x_i and v_i are phase-space variables corresponding to X_i and V_i, respectively.

For any variable such as f, the spatial filtering is defined by

$$\hat{f}(\mathbf{x}) = \int f(\mathbf{x}') H_\Delta(\mathbf{x} - \mathbf{x}')\,\mathrm{d}\mathbf{x}' \tag{5}$$

where $\hat{f}$ is referred as the filtered value of f and H_Δ is called the filter kernel function [15]. Here we take Δ as the smallest grid size required to fully resolve all scales of the carrier phase quantities; therefore, if g represents a typical carrier phase quantity, e.g., the carrier phase velocity, $\hat{g} = g$. In other words, Δ is set to a sufficiently small value that there are no subgrid scale fluctuations for the fluid phase and all scales of the fluid phase are fully resolved. For a turbulent flow, this small value is the limit at which LES is regarded as DNS. Applying Eq. (5) on Eq. (4), the filtered Liouville equation is obtained

$$\frac{\partial \hat{W}}{\partial t} + \frac{\partial v_i \hat{W}}{\partial x_i} - \frac{\partial}{\partial v_i}\left[\frac{(v_i - u_i)}{\tau} \hat{W}\right] = 0 \tag{6}$$

where $\hat{W}$ is the coarse-grained density function which has all properties of a probability density function if the kernel H_Δ is positive [16,17]. Examples of such kernels are top-hat and Gaussian filters.

The Eulerian variables for the particle phase are defined by

$$\bar{\phi}(\mathbf{x}, t) = \int \hat{W}(\mathbf{x}, \mathbf{v}, t)\,\mathrm{d}\mathbf{v} \tag{7}$$

Received 15 June 2010; revision received 4 October 2010; accepted for publication 5 October 2010.

*Assistant Professor, Department of Mechanical and Aerospace Engineering. Senior Member AIAA.

$$\bar{v}_i(\mathbf{x}, t) = \frac{1}{\bar{\phi}} \int v_i \hat{W}(\mathbf{x}, \mathbf{v}, t)\, d\mathbf{v} \tag{8}$$

where $\bar{\phi}$ and $\bar{v}_i$ represent the number density and Eulerian velocity of particles, respectively. By taking zero and first moments of Eq. (6) one obtains

$$\frac{\partial \bar{\phi}}{\partial t} + \frac{\partial \bar{\phi} \bar{v}_i}{\partial x_i} = 0 \tag{9}$$

$$\frac{\partial \bar{\phi} \bar{v}_i}{\partial t} + \frac{\partial \bar{\phi} \bar{v}_j \bar{v}_i}{\partial x_j} = -\frac{\partial \bar{\phi}(\overline{v_i v_j} - \bar{v}_i \bar{v}_j)}{\partial x_j} + \frac{1}{\tau} \bar{\phi}(u_i - \bar{v}_i) \tag{10}$$

where

$$\overline{v_i v_j} = \frac{1}{\bar{\phi}} \int v_i v_j \hat{W}(\mathbf{x}, \mathbf{v}, t)\, d\mathbf{v} \tag{11}$$

where $\overline{v_i v_j}$ is the second moment that gives rise to a closure problem similar to that encountered in Reynolds-averaged Navier–Stokes (RANS) modeling of turbulent flows [15]. A transport equation can be derived for $\overline{v_i v_j}$ by taking the second moments of Eq. (6)

$$\frac{\partial \bar{\phi}\, \overline{v_i v_j}}{\partial t} + \frac{\partial \bar{\phi}\, \overline{v_i v_j v_k}}{\partial x_k} = \frac{1}{\tau} \bar{\phi}(u_i \bar{v}_j + \bar{v}_i u_j - 2\overline{v_i v_j}) \tag{12}$$

where

$$\overline{v_i v_j v_k} = \frac{1}{\bar{\phi}} \int v_i v_j v_k W(\mathbf{x}, \mathbf{v}, t)\, d\mathbf{v} \tag{13}$$

To close the system of Eqs. (9), (10), and (12), third moments seen in Eq. (12) are approximated by

$$\overline{v_i v_j v_k} \approx \overline{v_j v_k} \bar{v}_i + \overline{v_i v_j} \bar{v}_k + \overline{v_i v_k} \bar{v}_j - 2\bar{v}_i \bar{v}_j \bar{v}_k \tag{14}$$

Proposed by Pandya and Mashayek [11], this approximation is second order as it is equivalent to setting the third cumulants equal to zero.

III. Model Assessment

Equations (9), (10), and (12), which are in a strong conservative form [18], constitute the three-dimensional Eulerian equations of particle Eulerian variables $\bar{\phi}$, $\bar{v}_k$, and $\overline{v_i v_j}$. They are coupled to each other and can be simultaneously solved along with the carrier phase Navier–Stokes equations governing u_i. In this work we focus on a 1-D problem as a first step toward model assessment assigning a known function to the fluid phase velocity assumed known in terms of x; therefore, no differential equations are required to solve for the fluid phase velocity to prevent further complexity in the preliminary assessment stage.

For a 1-D case, the particle-phase Eulerian Eqs. (9), (10), and (12), are simplified to

$$\frac{\partial \bar{\phi}}{\partial t} + \frac{\partial \bar{\phi}\, \bar{v}}{\partial x} = 0 \tag{15}$$

$$\frac{\partial \bar{\phi}\, \bar{v}}{\partial t} + \frac{\partial \bar{\phi} \bar{v}^2}{\partial x} = \frac{\partial \bar{\phi}(\bar{v}^2 - \overline{v^2})}{\partial x} + \frac{1}{\tau} \bar{\phi}(u - \bar{v}) \tag{16}$$

$$\frac{\partial \bar{\phi}\, \overline{v^2}}{\partial t} + \frac{\partial \bar{\phi}\, \overline{v^3}}{\partial x} = \frac{2}{\tau} \bar{\phi}(u\bar{v} - \overline{v^2}) \tag{17}$$

Following the approximation made in Eq. (14), $\overline{v^3}$ in Eq. (17) is approximated by

$$\overline{v^3} \approx 3\overline{v^2}\, \bar{v} - 2\bar{v}^3 \tag{18}$$

Incorporating above equation into Eq. (17), Eqs. (15–17) can be simplified to

$$\frac{\partial \mathbf{Q}}{\partial t} + \mathbf{A} \frac{\partial \mathbf{Q}}{\partial x} = \mathbf{S} \tag{19}$$

where

$$\mathbf{Q} = \begin{bmatrix} \bar{\phi} \\ \bar{v} \\ s \end{bmatrix}, \qquad \mathbf{A} = \begin{bmatrix} \bar{v} & \bar{\phi} & 0 \\ s/\bar{\phi} & \bar{v} & 1 \\ 0 & 2s & \bar{v} \end{bmatrix}, \qquad \mathbf{S} = \begin{bmatrix} 0 \\ (u - \bar{v})/\tau \\ -2s/\tau \end{bmatrix} \tag{20}$$

where $s = \overline{v^2} - \bar{v}^2$. The eigenvalues of $\mathbf{A}$, which are important for the numerical discretization of this system of equations, are obtained as $\lambda_1 = \bar{v}$, $\lambda_{2,3} = \bar{v} \pm \sqrt{3s}$. The hyperbolicity of Eq. (20) is in order when the eigenvalues are real [19], which is the case when s is positive. Positivity of the filter kernel H_Δ in Eq. (11) is a sufficient condition for a positive s [16].

Here, we consider a 1-D problem with a prescribed fluid velocity in the form of

$$u(x, t) = 1 + \beta \sin(2\pi k x) \tag{21}$$

Fluid-phase velocity seen in this equation nonlinearly varies with x, which is due to the second term on the right hand side of the equation. Furthermore, the particle time constant is set to unit and $\beta = 0.5$ in Eq. (21). Particles are released with an initial concentration that we consider to be a Gaussian function in space with an average at $x = 1$, and variance of 0.05. The initial velocity of particles are also Gaussian with a mean value of 1 and $s = s_0$. Therefore, the initial $\hat{W}$ is a bivariate Gaussian.

Equation (19) is solved using a first-order upwind finite difference scheme along with a first-order explicit Euler scheme in time [20]. Results obtained by the two-fluid model are compared against the results obtained by solving the Liouville Eq. (6) that is simplified to

$$\frac{\partial \hat{W}}{\partial t} + \frac{\partial v \hat{W}}{\partial x} - \frac{\partial}{\partial v}\left[\frac{(v - u)}{\tau} \hat{W}\right] = 0 \tag{22}$$

for a one-dimensional flow. Equation (22) is a linear first-order partial differential equation that is solved by the method of characteristics [19] in this work using the characteristics ordinary differential Eqs. (1) and (2). After solving for $\hat{W}(x, v, t)$, it can be integrated with respect to v to generate statistical quantities such as $\bar{\phi}$, $\bar{v}$ and $\overline{v^2}$ using Eqs. (7), (8), and (11).

IV. Results

Figure 1 shows the particle concentration versus space at various times. At time $t = 0$ we initialize the particle concentration with a

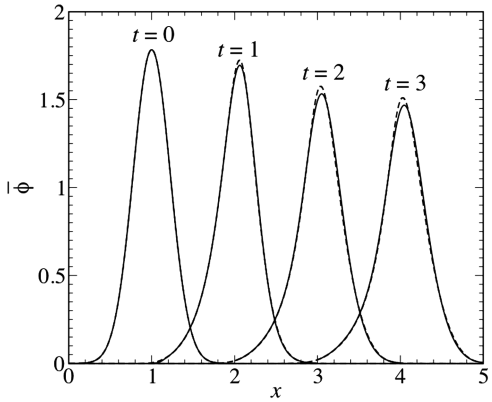

Fig. 1 Particle concentration at various times obtained by Liouville equation (solid line) and two-fluid model (dashed line) for $k = 1$ and $s_0 = 0.05$.

Gaussian function in x as shown in the figure. It is seen that with the increase of time the peak of $\bar{\phi}$ decreases and $\bar{\phi}$ broadens. The peaks at $t = 1, 2$, and 3 nearly correspond to $x = 2, 3$, and 4; however, a closer look to the concentration hills reveals that with the increase of time the initial hill becomes more asymmetric about the peak point and deviates from a Gaussian shape. A good agreement between the model and exact results at all times is observed in Fig. 1. The deviation between the two-fluid and Liouville equation solution is noticeable at the peaks of the curves. Shown results in Fig. 1 are obtained in a domain with boundaries at $x = -2$ and $x = 6$ with a grid size of $\Delta x = 2.5 \times 10^{-4}$ and a Courant–Friedrichs–Lewy (CFL) number of 0.5 where $\mathrm{CFL} = U_0 \Delta t / \Delta x$ with $U_0 = 1$ chosen according to the constant part of the fluid velocity given in Eq. (21).

Spatial and temporal convergence studies have been carried out for which results are shown in Fig. 2. The spatial discretization error $\varepsilon_{\Delta x} = \mathrm{mean}(|\bar{\phi}_{\Delta x} - \bar{\phi}_{\mathrm{finest}}|)$ where $\bar{\phi}_{\mathrm{finest}}$ corresponds to the finest spatial resolution with $\Delta x = 2.5 \times 10^{-4}$ and mean( ) is the mean carried out over all grid points. The temporal discretization error is $\varepsilon_{\Delta t} = \mathrm{mean}(|\bar{\phi}_{\Delta t} - \bar{\phi}_{\mathrm{finest}}|)$ where $\bar{\phi}_{\mathrm{finest}}$ corresponds to the smallest time step with $\Delta t = 3.125 \times 10^{-5}$. CPU times of the various resolutions are displayed in Fig. 3. All computations are performed on a Mac OS X with a 2.4 GHz Intel Core 2 Duo CPU and a 4 GB 1067 MHz DDR3 memory. The straight line seen in Fig. 3 has a slope of 2, meaning that CPU time $\propto N^2$.

Figure 4 shows the influence of the change of wave number k, seen in Eq. (21), and the variance of the initial particle-phase velocity s_0 on the spatial variation of the particle concentration. All other numerical and physical parameters are the same as those used in Fig. 1. The asymmetry of the particle concentration is the most visible in Fig. 3b which corresponds to the lowest wave number considered in this work. Very good agreements between the two-fluid model and Liouville equation results are seen in all cases shown in Fig. 3 with the best agreement in Fig. 3b corresponding to $k = 0.3$.

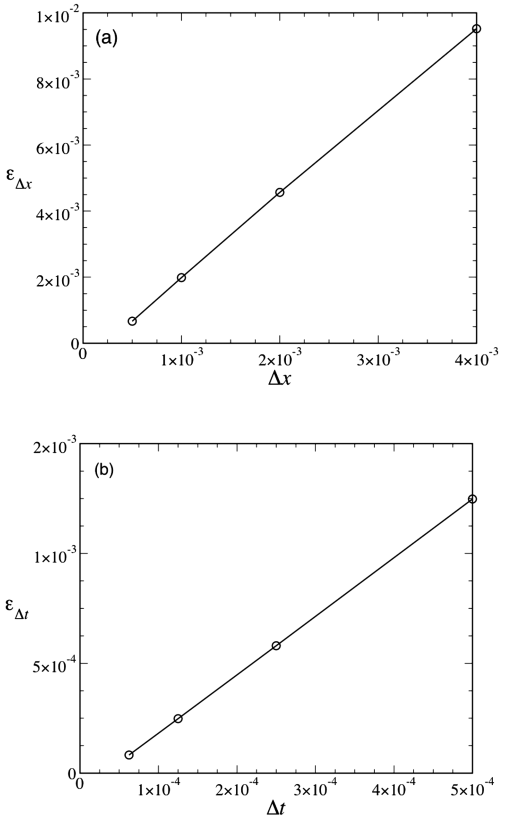

Fig. 2 Space and time discretization errors for $k = 1$ and $s_0 = 0.05$; (a) various space resolutions at fixed time step $\Delta t = 1.25 \times 10^{-4}$; (b) various time resolutions at fixed grid resolution $\Delta x = 1 \times 10^{-3}$.

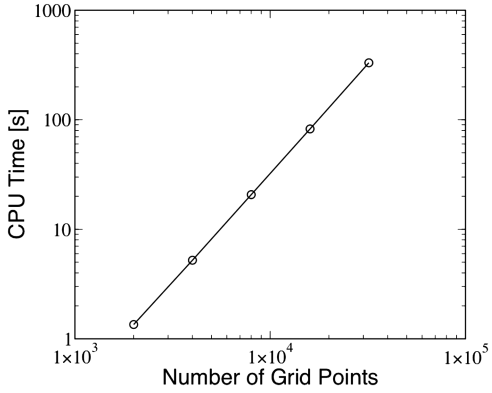

Fig. 3 Calculated CPU times versus the number of grid points for the two-fluid model code. The CFL = 0.5 is the same for all resolutions. $\mathrm{CFL} = U_0 \Delta t / \Delta x$ where $U_0 = 1$ according to the constant part of the velocity given in Eq. (21).

Figure 5 shows various statistics obtained by the Liouville equation and model solutions with the same physical and numerical parameters used for Fig. 1. These statistics represent the mean and variance of particle variables in a Lagrangian sense. These statistical variables for the two-fluid model are readily calculated from Eulerian variables through the following equations and they are only functions of time

$$\langle X \rangle = \int x \bar{\phi} \, \mathrm{d}x \tag{23}$$

$$\langle V \rangle = \int \bar{v} \, \bar{\phi} \, \mathrm{d}x \tag{24}$$

$$\langle X^2 \rangle = \int x^2 \bar{\phi} \, \mathrm{d}x - \langle X \rangle^2 \tag{25}$$

$$\langle V^2 \rangle = \int \overline{v^2} \, \bar{\phi} \, \mathrm{d}x - \langle V \rangle^2 \tag{26}$$

$$\langle XV \rangle = \int x \bar{v} \, \bar{\phi} \, \mathrm{d}x - \langle X \rangle \langle V \rangle \tag{27}$$

As seen in Fig. 5, all these statistics obtained by the model almost perfectly match those obtained by solving the Liouville equation.

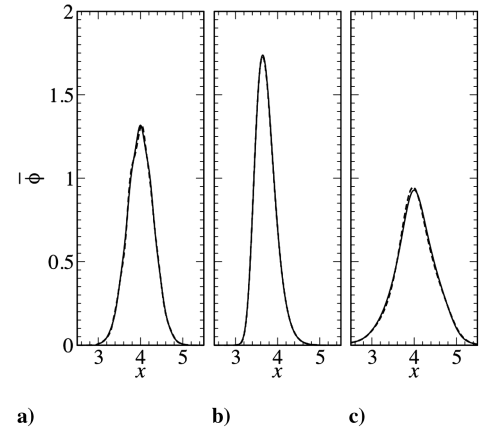

Fig. 4 Particle concentration at $t = 3$ for a) $k = 4$ and $s_0 = 0.05$; b) $k = 0.3$ and $s_0 = 0.05$; c) $k = 1$ and $s_0 = 0.2$. Liouville equation (solid line) and two-fluid model (dashed line).

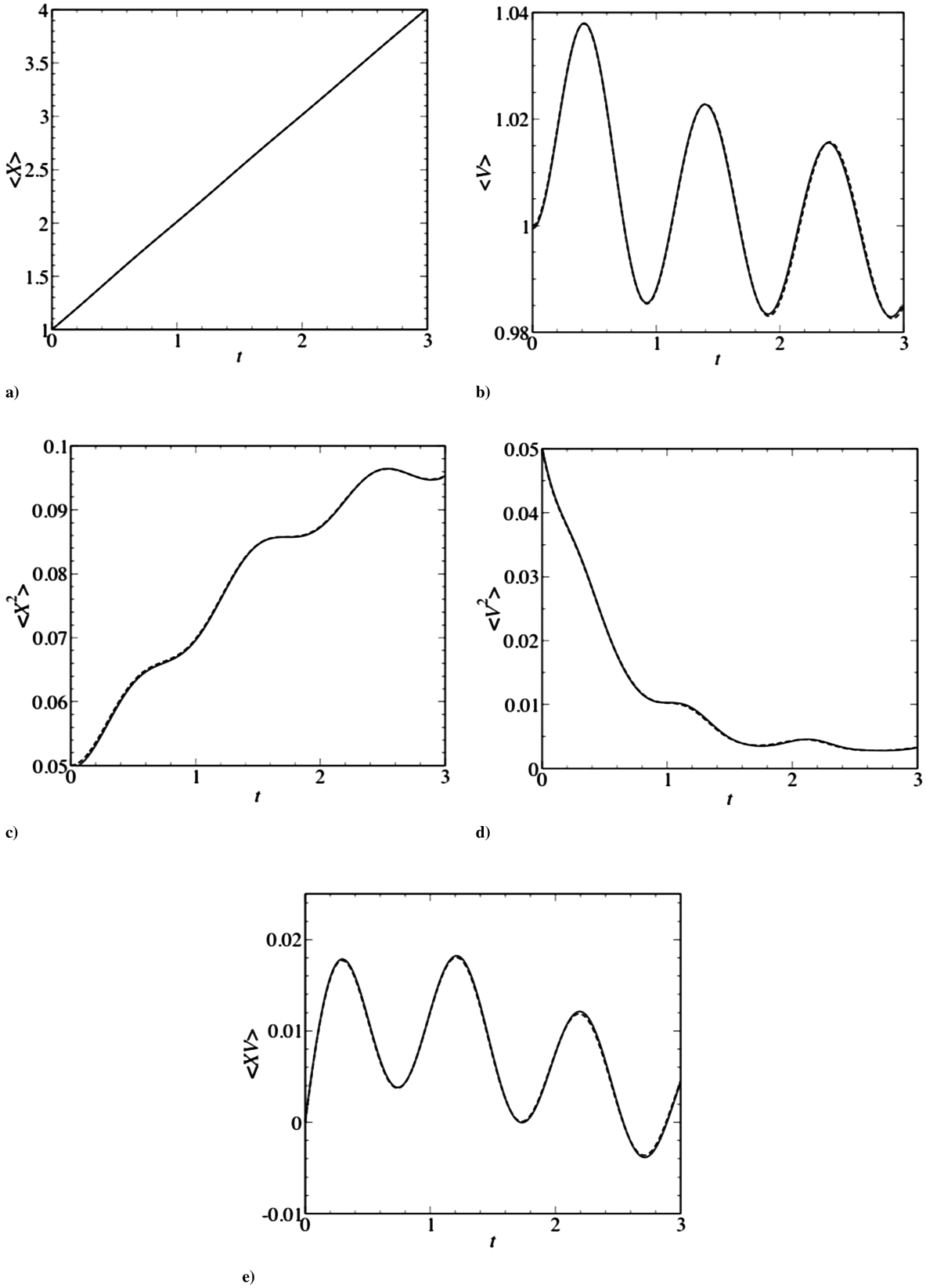

Fig. 5 Time evolution of various statistics obtained by Liouville equation (solid line) and two-fluid model (dashed line) for $k = 1$ and $s_0 = 0.05$.

V. Conclusions

The two-fluid model of Pandya and Mashayek [11], which is adapted for DNS and implemented in a 1-D sample problem, generates promising results as various statistical quantities obtained by the model are well compared against those obtained by directly solving the Liouville equation. The two-fluid model can be extended to the cases in which variation of temperature is important. To do so, a new phase-space variable representing the temperature of the particle can be added to the filtered density function. Consequently, additional transport equations for the first and second moments of temperature are obtained and need to be solved. Also in the case of two-way coupling, a source term that is a function of particle

concentration as well as the difference of the fluid and particle velocities can be added to the momentum equation of the fluid phase. A similar source term has been used in our recent study through equilibrium Eulerian approximation [10].

Further assessments of the model are required in 2-D and 3-D problems. In the sample problem the fluid phase velocity is prescribed; however, in the practical applications, the fluid phase velocity has to be solved in the Navier–Stokes equations. From numerical solution point of view, the compatibility between the fluid and particle solver has to be assured.

Acknowledgment

The author acknowledges the support provided by The University of Alabama in Huntsville through 2009 UA Huntsville Research Mini-Grant Program.

References

[1] Mashayek, F., and Pandya, R. V. R., "Analytical Description of Particle/Droplet-Laden Turbulent Flows," *Progress in Energy and Combustion Science*, Vol. 29, No. 4, 2003, p. 329. doi:10.1016/S0360-1285(03)00029-7

[2] Anderson, T. B., and Jackson, R., "A Fluid Mechanical Description of Fluidized Beds," *Industrial and Engineering Chemistry*, Vol. 6, No. 4, 1967, p. 527. doi:10.1021/i160024a007

[3] Jackson, R., "Locally Averaged Equations of Motion for a Mixture of Identical Spherical Particles and a Newtonian Fluid," *Chemical Engineering Science*, Vol. 52, No. 15, 1997, p. 2457. doi:10.1016/S0009-2509(97)00065-1

[4] Joseph, D. D., Lundgren, T. S., Jackson, R., and Saville, D. A., "Ensemble Averaged and Mixture Theory Equations for Incompressible Particle Suspension," *International Journal of Multiphase Flow*, Vol. 16, 1990, p. 35. doi:10.1016/0301-9322(90)90035-H

[5] Zhang, D. Z., and Prosperetti, A., "Momentum and Energy Equations for Disperse Two-Phase Flows and Their Closure for Dilute Suspensions," *International Journal of Multiphase Flow*, Vol. 23, No. 3, 1997, p. 425. doi:10.1016/S0301-9322(96)00080-8

[6] Ferry, J., and Balachandar, S., "A Fast Eulerian Method for Disperse Two-Phase Flow," *International Journal of Multiphase Flow*, Vol. 27, No. 7, 2001, p. 1199. doi:10.1016/S0301-9322(00)00069-0

[7] Maxey, M. R., "The Gravitational Settling of Aerosol Particles in Homogeneous Turbulence and Random Flow Fields," *Journal of Fluid Mechanics*, Vol. 174, No. -1, 1987, p. 441. doi:10.1017/S0022112087000193

[8] Shotorban, B., and Balachandar, S., "Particle Concentration in Homogeneous Shear Turbulence Simulated via Lagrangian and Equilibrium Eulerian Approaches," *Physics of Fluids*, Vol. 18, No. 6, 2006, p. 065105. doi:10.1063/1.2204982

[9] Shotorban, B., and Balachandar, S., "A Eulerian Model for Large-Eddy Simulation of Concentration of Particles with Small Stokes Numbers," *Physics of Fluids*, Vol. 19, No. 11, 2007, p. 118107. doi:10.1063/1.2804956

[10] Shotorban, B., and Balachandar, S., "Two-Fluid Approach for Direct Numerical Simulation of Particle-Laden Turbulent Flows at Small Stokes Numbers," *Physical Review E (Statistical Physics, Plasmas, Fluids, and Related Interdisciplinary Topics)*, Vol. 79, 2009, p. 056703. doi:10.1103/PhysRevE.79.056703

[11] Pandya, R. V. R., and Mashayek, F., "Two-Fluid Large-Eddy Simulation Approach for Particle-Laden Turbulent Flows," *International Journal of Heat and Mass Transfer*, Vol. 45, No. 24, 2002, p. 4753. doi:10.1016/S0017-9310(02)00191-6

[12] Balachandar, S., and Eaton, J. K., "Turbulent Dispersed Multiphase Flow," *Annual Review of Fluid Mechanics*, Vol. 42, No. 1, 2010, p. 111. doi:10.1146/annurev.fluid.010908.165243

[13] Balachandar, S., "A Scaling Analysis for Point–Particle Approaches to Turbulent Multiphase Flows," *International Journal of Multiphase Flow*, Vol. 35, 2009, p. 801. doi:10.1016/j.ijmultiphaseflow.2009.02.013

[14] Sengupta, K., Shotorban, B., Jacobs, G. B., and Mashayek, F., "Spectral-Based Simulations of Particle-Laden Turbulent Flows," *International Journal of Multiphase Flow*, Vol. 35, No. 9, 2009, p. 811. doi:10.1016/j.ijmultiphaseflow.2009.03.007

[15] Pope, S. B., *Turbulent Flows*, Cambridge Univ. Press, Cambridge, UK, 2000.

[16] Verman, B., Geurts, B., and Kuerten, H., "Realizability Conditions for the Turbulent Stress Tensor in Large-Eddy Simulation," *Journal of Fluid Mechanics*, Vol. 278, No. -1, 1994, p. 351. doi:10.1017/S0022112094003745

[17] Gicquel, L., Givi, P., Jaberi, F., and Pope, S., "Velocity Filtered Density Function for Large Eddy Simulation of Turbulent Flows," *Physics of Fluids*, Vol. 14, No. 3, 2002, p. 1196. doi:10.1063/1.1436496

[18] Ferziger, J. H., and Peric, M., *Computational Methods for Fluid Dynamics*, 3rd ed., Springer–Verlag, Berlin, 2002.

[19] Evans, L. C., *Partial Differential Equations*, 2nd ed., American Mathematical Society, Providence, RI, 2010.

[20] Fletcher, C. A. J., *Computational Techniques for Fluid Dynamics*, Vol. 2, Springer–Verlag, Berlin, 1988.

T. Jackson
Associate Editor